

Numerical Simulation of Forest Fires Based on 2D Model

A.A. KULESHOV, E.E. MYSHETSKAYA

Keldysh Institute of Applied Mathematics

of Russian Academy of Sciences

Miuskaya sq., 4, Moscow, 125047

RUSSIA

andrew_kuleshov@mail.ru

Abstract: - The problem of numerical simulation of forest fires is considered. A two-dimensional two-phase mathematical model, the numerical method and the results of a demonstrative numerical simulation of the process of forest fire spread are presented.

Key-Words: - Forest fire, mathematical model, numerical method, numerical simulation

1 Introduction

Forest fire is a complex natural phenomenon for which various mathematical modeling approaches have been proposed. For example, some of them for the computation of the forest fire front dynamics use models of cellular automatic machines [1, 2]. However the most part of the forest fire models used today based on the gas dynamics equations. Two-dimensional (x,z) -models are used to computation forest fire spread in a specified direction [3, 4], but this models fail to produce a correct description of a real forest fire when the forest fuel materials are distributed non-homogeneously. There is still another wide range of models focusing on some particular phenomena observed in the forest fire zone and in the atmosphere above it, e.g., thermals ascent and buoyant plums forming. The majority of them are based on two-dimensional axisymmetric models [3]. Coherent vertical structures in the atmosphere above a forest fire are computed based on three-dimensional models [5, 6]. Other studies [7-9] deal with the three-dimensional single-phase gas-dynamic forest fire model ignoring chemical reactions and approximating the upward thermal energy fluxes by means of an analytical formula and radiant energy transfer is not considered.

Turbulent flows arising during real forest fires have a complex three-dimensional character and their numerical simulation on the basis of three-dimensional models demands the long time of computation and supercomputer applications. However, for an operative estimation and forecasting of process of fire spreading, models are needed that can enable to carry out fast computations of this process dynamics. In the development of such models, it is expedient to use simplified two-dimensional problem statements

taking into account the features appropriate to the process under consideration. A two-dimensional two-phase mathematical model of forest fires developed by the authors [10, 11] is considered below. The model is based on the averaging of three-dimensional set of equations over the thickness of the homogeneous forest fuel materials (FFM) layer. Nevertheless, these models reflect the fundamental physical laws of conservation of mass, momentum and energy and take into account all of the physical phenomena in the fire zone that are important for the fire dynamics. On the basis of this single-layer model it is possible to construct more complex many-layer models of forest fires. Numerical method by splitting the system of equations by physical processes into several subsystems with the finite-difference approximation of this subsystems and the results of a demonstrative numerical simulation of the process of forest fire spread are presented below.

2 Two-phase Forest Fire Model

2.1 Phase and Chemical Composition

The proposed two-phase model treats a forest as a single-storey two-phase medium consisting of air and gaseous products of pyrolysis and combustion (the air-gas or gas phase) and FFM with solid products of pyrolysis (solid phase). In this model, the two-phase heterogeneous mixture is considered as a two-component continuum with mass, momentum and energy exchange between the phases. The gas phase is a medium composed by six components: combustible gas CO (mass concentration C_1), oxidizer O_2 (C_2), carbon dioxide

CO₂ (C₃), water vapor H₂O (C₄), nitrogen N₂ (C₅), and dispersed soot (C_s). Our assumption is that the disperse soot particles move together with the gas phase and when the soot particles are burned, the heat exchange process is so rapid that we can characterize it by the only temperature of the gas phase. The solid phase is also a multicomponent medium composed by the FFM (volume fraction φ₁) and products of FFM pyrolysis: breeze coke (φ₂) and ashes (φ₃). Breeze coke and disperse soot consist of virtually 100 percent of carbon and are burned up completely.

2.2 Set of Equations

Let's consider a single-layer model of forest fire in a layer of FFM of constant thickness; it is supposed that all physical and chemical parameters in this layer are approximately equal to some average values for this layer.

The equation set of the two-phase, two-dimensional, single-layer model obtained by integrating the original three-dimensional equations over the FFM layer height has the form:

gas phase:

$$\frac{\partial \rho}{\partial t} + \frac{\partial \rho u}{\partial x} + \frac{\partial \rho v}{\partial y} = Q - J_{\rho}, \quad (1)$$

$$\frac{\partial \rho u}{\partial t} + \frac{\partial (\rho u^2 + \phi p)}{\partial x} + \frac{\partial \rho uv}{\partial y} = p \frac{\partial \phi}{\partial x} + \quad (2)$$

$$+ \frac{\partial}{\partial x} \left(\mu_{eff} \frac{\partial u}{\partial x} \right) + \frac{\partial}{\partial y} \left(\mu_{eff} \frac{\partial u}{\partial y} \right) + F_1 + F_1^0 - J_u,$$

$$\frac{\partial \rho v}{\partial t} + \frac{\partial (\rho v^2 + \phi p)}{\partial x} + \frac{\partial \rho uv}{\partial y} = p \frac{\partial \phi}{\partial y} + \quad (3)$$

$$+ \frac{\partial}{\partial x} \left(\mu_{eff} \frac{\partial v}{\partial x} \right) + \frac{\partial}{\partial y} \left(\mu_{eff} \frac{\partial v}{\partial y} \right) + F_2 + F_2^0 - J_v,$$

$$\frac{\partial \rho E}{\partial t} + \frac{\partial (\rho u E + \phi p u)}{\partial x} + \frac{\partial (\rho v E + \phi p v)}{\partial y} = \quad (4)$$

$$= \frac{\partial}{\partial x} \left(k_{eff} \frac{\partial T}{\partial x} \right) + \frac{\partial}{\partial y} \left(k_{eff} \frac{\partial T}{\partial y} \right) + p \sum_{j=1}^3 \left(R_{\phi_j} / \rho_j \right) +$$

$$+ \alpha (T_1 - T) + \sigma (\alpha_1 T_1^4 - \alpha T^4) + f_{\Gamma} + f_{\Gamma R} + Q_T - J_E,$$

$$\frac{\partial \rho C_i}{\partial t} + \frac{\partial \rho u C_i}{\partial x} + \frac{\partial \rho v C_i}{\partial y} = R_{C_i} - J_{C_i} + \quad (5)$$

$$+ \frac{\partial}{\partial x} \left(\rho D_{eff} \frac{\partial C_i}{\partial x} \right) + \frac{\partial}{\partial y} \left(\rho D_{eff} \frac{\partial C_i}{\partial y} \right), \quad i = \overline{1,5},$$

$$\frac{\partial \rho C_s}{\partial t} + \frac{\partial \rho u C_s}{\partial x} + \frac{\partial \rho v C_s}{\partial y} = R_{C_s} - J_{C_s}, \quad (6)$$

$$p = \hat{\rho} R T \sum_{i=1}^5 \frac{C_i}{M_i}; \quad (7)$$

solid phase:

$$\rho_j \frac{\partial \phi_j}{\partial t} = R_{\phi_j}, \quad j = \overline{1,3}, \quad (8)$$

$$\frac{\partial}{\partial t} \sum_{j=1}^3 \rho_j \phi_j c_{pj} T_1 = -p \sum_{j=1}^3 \left(R_{\phi_j} / \rho_j \right) - \quad (9)$$

$$- \alpha (T_1 - T) - \sigma (\alpha_1 T_1^4 - \alpha T^4) + Q_{T_1};$$

normalization and balance relations:

$$\phi + \sum_{j=1}^3 \phi_j = 1, \quad \sum_{i=1}^5 C_i + C_s = 1, \quad (10)$$

$$\sum_{i=1}^5 R_{C_i} + R_{C_s} = Q, \quad \sum_{j=1}^3 R_{\phi_j} = -Q.$$

The system (1)-(10) is considered in Cartesian coordinates in a rectangular area $\Omega = \{0 \leq x \leq l_1, 0 \leq y \leq l_2\}$ on a horizontal plane XY , ρ is the partial density of the gas phase, p is the total pressure of the multiphase medium, $\mathbf{V} = (u, v)$ is velocity of the gas phase, T is the gas phase temperature, E is the total energy of the gas phase, $E = 0.5(u^2 + v^2) + c_v T$, c_v is the gas specific heat capacity at constant volume, ϕ is the volume fraction of the gas phase, $\mathbf{F} = -\rho c_d s \mathbf{V} |\mathbf{V}|$ is the volume force related to the exchange of momentum between the phases (the force of friction between the phases), c_d is an empirical drag coefficient for forest vegetation, s is the FFM specific surface area, $\mathbf{F}^0 = -\rho \xi_0 (\mathbf{V} - \mathbf{V}_0) |\mathbf{V} - \mathbf{V}_0|$ is the wind influence

on the top border of the FFM layer, V_0 is the wind velocity, ξ_0 is a non-dimensional empirical coefficient of friction between the gas in the forest layer and in the atmosphere at the top boundary of the forest layer, Q is the mass source describing the gas inflow due to the processes taking place in the solid phase, Q_T is the heat generation in the gas phase, R_{C_i} is the rate of ρC_i variation due to chemical reactions, R_{C_s} is the rate of ρC_s variation due to chemical reactions, $J_\rho, J_u, J_v, J_C, J_s, J_E$ are the mass, momentum and energy fluxes at the upper and lower boundaries of the FFM layer, $\hat{\rho} = \rho/\phi$ is the real density of the gas phase, R is the universal gas constant, M_i are the molecular masses of the gas phase components, $\rho_j, j = \overline{1,3}$ are the real densities of solid phase components, $c_{pj}, j = \overline{1,3}$ are the solid phase components' heat capacities, $R_{\phi_j}, j = \overline{1,3}$ is the rate of the volume fraction ϕ_j variation as a result of chemical reactions, T_1 is the solid phase temperature, Q_{T_1} is the heat generation in the solid phase.

2.3 Turbulence Closure

The effective viscosity μ_{eff} is the sum of the laminar μ_l and turbulent μ_t components, $\mu_{eff} = \mu_l + \mu_t$, the laminar viscosity is calculated from Sutherland's formula. The two-dimensional analog of the three-dimensional algebraic turbulence model [12] for the proposed description of turbulent viscosity is used

$$\mu_t = \rho l^2 \left\{ 2 \left[\left(\frac{\partial u}{\partial x} \right)^2 + \left(\frac{\partial v}{\partial y} \right)^2 \right] + \left(\frac{\partial u}{\partial y} + \frac{\partial v}{\partial x} \right)^2 \right\}^{1/2},$$

where mixing distance l can be determined as the FFM layer thickness h .

The total heat conductivity coefficient takes into account the heat and the turbulent heat conductivity as well as heat transfer by radiative conduction [13, 14], $k_{eff} = k_l + k_t + k_r$ where $k_l = c_p \mu_l / Pr$ is the heat conductivity coefficient, $k_t = c_p \mu_t / Pr_t$ is the turbulent heat conductivity coefficient, $Pr = Pr_t = 0.7$ are the laminar and turbulent the Prandtl numbers, $k_r = 16 \sigma l_s T^3 / 3$ is the radiative heat conductivity, l_s is the radiation mean path, σ is

the Stefan-Boltzmann constant. The effective diffusion coefficient is defined as $D_{eff} = \mu_l / \rho Sc + \mu_t / \rho Sc_t$, where $Sc = Sc_t = 0.7$ are the laminar and turbulent Schmidt numbers.

2.4 Chemical Processes in a Gas and Solid Phases

To consider the fundamental chemical reactions [3] let us take reactions of the FFM pyrolysis (defined as the speed of reaction – R_0), carbon oxide burning (R_1), breeze coke burning (R_c) and dispersed soot burning (R_s). The speeds of the fundamental chemical reactions are described by the Arrhenius law. The speeds of the chemical reactions $R_{C_i}, R_{C_s}, R_{\phi_j}$ are described by the speeds of the fundamental chemical reactions.

The heat generation in the gas phase is the sum of the heat generation in combustion of the carbon oxide and combustion of the dispersed soot $Q_T = q_1 R_1 + q_c R_s$ where q_1 is the carbon oxide combustion heat and q_c is the carbon combustion heat. The heat generation in combustion of the breeze coke $Q_{T_1} = q_c R_c$.

2.5 Mass, Momentum and Energy Fluxes at the Upper and Lower Boundaries of the FFM Layer

The mass, momentum and energy fluxes at the upper and lower boundaries of the FFM layer $J_\rho, J_u, J_v, J_E, J_C, J_{C_s}$ are described by the formula

$$J_\Phi = \frac{\Phi w|_{z=h_2}}{h} - \frac{\Phi w|_{z=h_1}}{h},$$

$$\Phi = (\rho, \rho u, \rho v, \rho E, \rho C, \rho C_s)^T$$

where h_1 and h_2 are the heights of the FFM layer lower and upper boundaries respectively, $h = h_2 - h_1$ is the FFM layer thickness, and the vertical velocity w at the upper FFM layer boundary is determined from a semi-empirical formula [3], $w|_{z=h_2} = (g(T - T_2)h / T_2)^{1/2}$, T_2 is temperature above the upper FFM layer boundary. For a fire in crowns of trees T_2 is temperature of the surrounding atmosphere. In the single-layer model being considered, we have $w|_{z=h_1} = 0$. For the two-layer model, the value of $w|_{z=h_1}$ for the upper FFM layer is taken to be equal to $w|_{z=h_2}$ for the lower layer.

2.6 Interphase Heat and Radiant Energy Exchange

The interphase heat energy exchange is described by the formula $\alpha(T_1 - T)$, where α is the heat exchange coefficient; f_Γ is the heat exchange at the upper and lower boundaries of the FFM layer which is described by the similar formula.

The interphase radiant energy exchange is described by the formula $\sigma(\alpha_1 T_1^4 - \alpha T^4)$, where α is the radiation gas absorption coefficient, α_1 is the radiation solid phase absorption coefficient; $f_{\Gamma R}$ is the radiant energy exchange at the upper and lower FFM layer boundaries which is described by the similar formula.

2.7 Boundary and Initial Conditions

The boundary conditions for the system of equations (1)-(10) must be supplied on all open boundaries of the computational domain. On the inflow boundary parts the following relation is used (here the subscript a refers to the atmospheric values)

$$\Phi|_\Gamma = \Phi_a, \quad \Phi = (\rho, u, v, T)^T, \quad (\mathbf{V}, \mathbf{n}) \leq 0;$$

on the outflow boundary parts

$$\frac{\partial \Phi}{\partial \mathbf{n}}|_\Gamma = 0, \quad \Phi = (\rho, u, v, E, C)^T, \quad (\mathbf{V}, \mathbf{n}) > 0.$$

The initial values of these parameters are set to the parameters of the surrounding atmosphere; in the fire source the values characteristic for the given fire and FFM type are specified: (T^0, T_1^0, C^0, C_s^0) , the initial velocity is equal to zero ($\mathbf{V}^0 = 0$), and initial pressure set equal to the atmospheric ($p^0 = p_a$) as it is known that pressure reaches its equilibrium state in any open system. The initial density of the gas phase is obtained from the equation of state (7).

3 Numerical Method

3.1 Method of splitting by physical processes

For numerical solution of the problem the efficient algorithm of splitting by physical processes has been used. A discretization in time $t_{n+1} = t_n + \Delta t$ is considered. At the time step $[t_n, t_{n+1}]$ the system (1)-(10) splits to the following stages (input data for the each stage are obtained at the previous stage):

The 1st stage: gas phase transfer

$$\frac{\partial \Phi}{\partial t} + \frac{\partial \mathbf{G}(\Phi)}{\partial x} + \frac{\partial \mathbf{H}(\Phi)}{\partial y} = 0, \tag{11}$$

where

$$\Phi = \begin{pmatrix} \rho \\ \rho u \\ \rho v \\ \rho E \\ \rho C \\ \rho C_s \end{pmatrix}, \quad \mathbf{G}(\Phi) = \begin{pmatrix} \rho u \\ \rho u^2 + \phi p \\ \rho u v \\ \rho u E + \phi p u \\ \rho u C \\ \rho u C_s \end{pmatrix}, \quad \mathbf{H}(\Phi) = \begin{pmatrix} \rho v \\ \rho u v \\ \rho v^2 + \phi p \\ \rho v E + \phi p v \\ \rho v C \\ \rho v C_s \end{pmatrix}.$$

The 2nd stage: accounting for the leaving of the substation at the upper boundary of the FFM layer

$$\frac{\partial \rho u}{\partial t} = p \frac{\partial \phi}{\partial x}, \quad \frac{\partial \rho v}{\partial t} = p \frac{\partial \phi}{\partial y}.$$

After that stage are calculated values:

$$u = \frac{\rho u}{\rho}, \quad v = \frac{\rho v}{\rho}, \quad E = \frac{\rho E}{\rho}, \quad C = \frac{\rho C}{\rho},$$

$$C_s = \frac{\rho C_s}{\rho}, \quad T = \frac{1}{c_v} \left(E - \frac{u^2}{2} - \frac{v^2}{2} \right).$$

The 3th stage: accounting for the interphase friction

$$\frac{\partial \mathbf{V}}{\partial t} = -c_d s \mathbf{V} |\mathbf{V}|, \quad \mathbf{V} = (u, v)^T. \tag{12}$$

The 4th stage: accounting for wind velocity blowing through a forest canopy

$$\frac{\partial \mathbf{V}}{\partial t} = -\xi_0 (\mathbf{V} - \mathbf{V}_0) |\mathbf{V} - \mathbf{V}_0|. \tag{13}$$

The 5th stage: accounting for turbulent viscosity, heat conductivity, and diffusion

$$\frac{\partial u}{\partial t} = \frac{\partial \tilde{\tau}_{xx}}{\partial x} + \frac{\partial \tilde{\tau}_{yx}}{\partial y}, \quad \frac{\partial v}{\partial t} = \frac{\partial \tilde{\tau}_{xy}}{\partial x} + \frac{\partial \tilde{\tau}_{yy}}{\partial y},$$

$$\frac{\partial T}{\partial t} = \frac{\partial}{\partial x} \left(\tilde{k}_{eff} \frac{\partial T}{\partial x} \right) + \frac{\partial}{\partial y} \left(\tilde{k}_{eff} \frac{\partial T}{\partial y} \right), \tag{14}$$

$$\frac{\partial C}{\partial t} = \frac{\partial}{\partial x} \left(D_{eff} \frac{\partial C}{\partial x} \right) + \frac{\partial}{\partial y} \left(D_{eff} \frac{\partial C}{\partial y} \right),$$

where

$$\tilde{\tau}_{ki} = v_{eff} \left(\frac{\partial v_k}{\partial x_i} + \frac{\partial v_i}{\partial x_k} - \frac{2}{3} \delta_{ki} \frac{\partial v_l}{\partial x_l} \right),$$

$$v_{eff} = \mu_{eff} / \rho, \quad \tilde{k}_{eff} = \frac{k_{eff}}{c_v \rho}.$$

The 6th stage: accounting for chemical reactions

Mass and the volume fraction variation as a result of chemical reactions:

$$\frac{\partial \rho}{\partial t} = Q, \quad \rho_l \frac{\partial \phi_l}{\partial t} = R_{\phi_l}, \quad l = \overline{1,3}, \quad \phi = 1 - \sum_{l=1}^3 \phi_l,$$

$$\frac{\partial \rho C_j}{\partial t} = R_{C_j}, \quad j = \overline{1,4}, \quad \frac{\partial \rho C_s}{\partial t} = R_{C_s},$$

$$C_5 = 1 - \sum_{j=1}^4 C_j - C_s.$$

Heat variation in the gas and solid phases as a result of chemical reactions:

$$\frac{\partial \rho c_v T}{\partial t} = p \sum_{l=1}^3 (R_{\phi_l} / \rho_l) + Q_T,$$

$$\frac{\partial}{\partial t} \sum_{l=1}^3 \rho_l \phi_l c_{pl} T_1 = -p \sum_{l=1}^3 (R_{\phi_l} / \rho_l) + Q_{T_1}.$$

The 7th stage: accounting for interphase heat exchange and exchange by radiant energy

$$\frac{\partial \rho c_v T}{\partial t} = \alpha (T_1 - T) + \sigma (\alpha_1 T_1^4 - \alpha T^4) + f_{\Gamma} + f_{\Gamma R},$$

$$\frac{\partial}{\partial t} \sum_{l=1}^3 \rho_l \phi_l c_{pl} T_1 = -\alpha (T_1 - T) - \sigma (\alpha_1 T_1^4 - \alpha T^4).$$

The 8th stage: accounting the mass, momentum and energy fluxes at the upper and lower boundaries of the FFM layer

$$\frac{\partial \Phi}{\partial t} = -\mathbf{J}_{\Phi}.$$

The 9th stage: accounting the pressure from the equation of state

$$p = \hat{\rho} RT \sum_{j=1}^5 \frac{C_j}{M_j}.$$

3.2 Finite-difference approximation

On each stage the subsystems are solved using a finite-difference method on a rectangular mash. Scheme TVD [11] was applied to the solution of a subsystem (11):

$$\Phi_{ij}^{n+1} = \Phi_{ij}^n - \frac{\Delta t}{\Delta x} (\mathbf{G}_{i+1/2,j}^n - \mathbf{G}_{i-1/2,j}^n) - \frac{\Delta t}{\Delta y} (\mathbf{H}_{i,j+1/2}^n - \mathbf{H}_{i,j-1/2}^n), \quad i = \overline{2, N_1 - 1}, \quad j = \overline{2, N_2 - 1}.$$

where

$$\mathbf{G}_{i+1/2,j}^n = \frac{\mathbf{G}(\Phi_{i+1/2,j}^L) + \mathbf{G}(\Phi_{i+1/2,j}^R)}{2} - D_{i+1/2,j}^u \frac{\Phi_{i+1/2,j}^R - \Phi_{i+1/2,j}^L}{2},$$

$$\mathbf{G}(\Phi_{i+1/2,j}^L) = \begin{pmatrix} \rho_{i+1/2,j}^L u_{i+1/2,j}^L \\ \rho_{i+1/2,j}^L (u_{i+1/2,j}^L)^2 + p_{i+1/2,j}^L \\ \rho_{i+1/2,j}^L u_{i+1/2,j}^L v_{i+1/2,j}^L \\ \rho_{i+1/2,j}^L u_{i+1/2,j}^L E_{i+1/2,j}^L + p_{i+1/2,j}^L u_{i+1/2,j}^L \\ \rho_{i+1/2,j}^L u_{i+1/2,j}^L \mathbf{C}_{i+1/2,j}^L \\ \rho_{i+1/2,j}^L u_{i+1/2,j}^L \mathbf{C}_{s i+1/2,j}^L \end{pmatrix},$$

$$E_{i+1/2,j}^L = \frac{1}{2} \left((u_{i+1/2,j}^L)^2 + (v_{i+1/2,j}^L)^2 \right) + c_v T_{i+1/2,j}^L,$$

$$D_{i+1/2,j}^u = \max \{ |u_{i+1/2,j}^L| + c_{i+1/2,j}^L, |u_{i+1/2,j}^R| + c_{i+1/2,j}^R \},$$

$c_{i+1/2,j}^L = (\gamma(\gamma-1)c_v T_{i+1/2,j}^L)^{1/2}$ is the finite-difference approximation of sound speed, γ is adiabatic index,

$$p_{i+1/2,j}^L = p(\rho_{i+1/2,j}^L, T_{i+1/2,j}^L, \mathbf{C}_{i+1/2,j}^L);$$

functions $\mathbf{G}(\Phi_{i+1/2,j}^R), E_{i+1/2,j}^R, \mathbf{C}_{i+1/2,j}^R, p_{i+1/2,j}^R$ are described by the similar formulas.

For the function $\Psi = (\rho, u, v, w, T, C, C_s)^T$:

$$\Psi_{i+1/2,j}^L = \Psi_{ij} + \left\langle \frac{\partial \Psi}{\partial x} \right\rangle_i \frac{\Delta x}{2}, \quad i = \overline{2, N_1 - 1},$$

$$\Psi_{i+1/2,j}^R = \Psi_{i+1,j} - \left\langle \frac{\partial \Psi}{\partial x} \right\rangle_{i+1} \frac{\Delta x}{2}, \quad i = \overline{1, N_1 - 2},$$

$$\left\langle \frac{\partial \Psi}{\partial x} \right\rangle_i = \begin{cases} 0, \text{ if } \frac{\Psi_{i+1,j} - \Psi_{ij}}{\Delta x} \text{ and } \frac{\Psi_{ij} - \Psi_{i-1,j}}{\Delta x} \text{ have} \\ \text{different signs; if signs are equal:} \\ \frac{\Psi_{i+1,j} - \Psi_{ij}}{\Delta x}, \text{ if } \left| \frac{\Psi_{i+1,j} - \Psi_{ij}}{\Delta x} \right| \leq \left| \frac{\Psi_{ij} - \Psi_{i-1,j}}{\Delta x} \right|, \\ \frac{\Psi_{ij} - \Psi_{i-1,j}}{\Delta x}, \text{ if } \left| \frac{\Psi_{i+1,j} - \Psi_{ij}}{\Delta x} \right| > \left| \frac{\Psi_{ij} - \Psi_{i-1,j}}{\Delta x} \right|, \end{cases}$$

$$i = \overline{2, N_1 - 1},$$

$$\Psi_{3/2,j}^L = \Psi_{5/2,j}^L, \quad \Psi_{N_1-1/2,j}^R = \Psi_{N_1-3/2,j}^R.$$

$$\mathbf{H}_{i,j+1/2}^n = \frac{\mathbf{H}(\Phi_{i,j+1/2}^L) + \mathbf{H}(\Phi_{i,j+1/2}^R)}{2} -$$

$$-D_{i,j+1/2}^v \frac{\Phi_{i,j+1/2}^R - \Phi_{i,j+1/2}^L}{2},$$

$$\mathbf{H}(\Phi_{i,j+1/2}^L) = \begin{pmatrix} \rho_{i,j+1/2}^L v_{i,j+1/2}^L \\ \rho_{i,j+1/2}^L u_{i,j+1/2}^L v_{i,j+1/2}^L \\ \rho_{i,j+1/2}^L (v_{i,j+1/2}^L)^2 + p_{i,j+1/2}^L \\ \rho_{i,j+1/2}^L v_{i,j+1/2}^L E_{i,j+1/2}^L + p_{i,j+1/2}^L v_{i,j+1/2}^L \\ \rho_{i,j+1/2}^L v_{i,j+1/2}^L \mathbf{C}_{i,j+1/2}^L \\ \rho_{i,j+1/2}^L v_{i,j+1/2}^L C_{si,j+1/2}^L \end{pmatrix}$$

$$E_{i+1/2,j}^L = \frac{1}{2} \left((u_{i+1/2,j}^L)^2 + (v_{i+1/2,j}^L)^2 \right) + c_v T_{i+1/2,j}^L,$$

$$D_{i,j+1/2}^v = \max \{ |v_{i,j+1/2}^L| + c_{i,j+1/2}^L, |v_{i,j+1/2}^R| + c_{i,j+1/2}^R \},$$

$$c_{i,j+1/2}^L = (\gamma(\gamma - 1) c_{v,i,j+1/2}^L)^{1/2},$$

$$p_{i,j+1/2}^L = p(\rho_{i,j+1/2}^L, T_{i,j+1/2}^L, C_{i,j+1/2}^L);$$

functions

$$\mathbf{H}(\Phi_{i,j+1/2}^R), E_{i,j+1/2}^R, c_{i,j+1/2}^R, p_{i,j+1/2}^R$$

are described by the similar formulas.

$$\Psi_{i,j+1/2}^L = \Psi_{ij} + \left\langle \frac{\partial \Psi}{\partial y} \right\rangle_j \frac{\Delta y}{2}, \quad j = \overline{2, N_2 - 1},$$

$$\Psi_{i,j+1/2}^R = \Psi_{i,j+1} - \left\langle \frac{\partial \Psi}{\partial y} \right\rangle_{j+1} \frac{\Delta y}{2}, \quad j = \overline{1, N_2 - 2},$$

$$\left\langle \frac{\partial \Psi}{\partial y} \right\rangle_j = \begin{cases} 0, \text{ if } \frac{\Psi_{i,j+1} - \Psi_{ij}}{\Delta y} \text{ and } \frac{\Psi_{ij} - \Psi_{i,j-1}}{\Delta y} \text{ have} \\ \text{different signs; if signs are equal:} \\ \frac{\Psi_{i,j+1} - \Psi_{ij}}{\Delta y}, \text{ if } \left| \frac{\Psi_{i,j+1} - \Psi_{ij}}{\Delta y} \right| \leq \left| \frac{\Psi_{ij} - \Psi_{i,j-1}}{\Delta y} \right| \\ \frac{\Psi_{ij} - \Psi_{i,j-1}}{\Delta y}, \text{ if } \left| \frac{\Psi_{i,j+1} - \Psi_{ij}}{\Delta y} \right| > \left| \frac{\Psi_{ij} - \Psi_{i,j-1}}{\Delta y} \right| \end{cases}$$

$$j = \overline{2, N_2 - 1},$$

$$\Psi_{i,3/2}^L = \Psi_{i,5/2}^L, \quad \Psi_{i,N_2-1/2}^R = \Psi_{i,N_2-3/2}^R.$$

This finite-difference scheme is of the first order by t and of the second order by x and y , and the stability condition has a form:

$$\max_{ij} (|\mathbf{V}_{ij}| + c_{ij}) \frac{\Delta t}{\min(\Delta x, \Delta y)} < \frac{1}{4}.$$

The solution of the subsystems (12) and (13) has been received analytically. The solution of the subsystem (12) on $[t_n, t_{n+1}]$ has a form:

$$u^{n+1} = \frac{u^n}{1 + c_d s |\mathbf{V}^n| \Delta t},$$

$$v^{n+1} = \frac{v^n}{1 + c_d s |\mathbf{V}^n| \Delta t}.$$

The solution of the subsystem (13) has a form:

$$u^{n+1} = \frac{u^n + \xi_0 u_0 |\mathbf{V}^n - \mathbf{V}_0| \Delta t}{1 + \xi_0 |\mathbf{V}^n - \mathbf{V}_0| \Delta t},$$

$$v^{n+1} = \frac{v^n + \xi_0 v_0 |\mathbf{V}^n - \mathbf{V}_0| \Delta t}{1 + \xi_0 |\mathbf{V}^n - \mathbf{V}_0| \Delta t}.$$

Then these solutions have been approximated by explicit schemes.

The subsystem (14) can be solved by means of effective multigrid method [15, 16]. To the solution of other subsystems the explicit schemes were used too.

4 Results of Numerical Simulation

Numerical simulation of the process of fire spread is carried out on the mesh with 1000×1000 points. Computations on this mesh only one step on time for the PC lasts 5 minutes therefore for the numerical simulation of the process a supercomputer been used. The parallel software has been written in FORTRAN using the MPI library and based on a well known method of geometrical parallelism. Computations using 400 processors on the supercomputer MVS 15000 in Russian Academy of Sciences have been performed.

Figure 1 shows the results of a demonstrative numerical simulation of a forest fire spreading in one-layer of the FFM under the action of the wind blowing through it at a speed $\mathbf{V}_0 = (2, -2)$ m/s and with the assumption that the FFM are distributed non-homogeneously. Initially, the source of the fire has the shape of a circle. Figure 1a shows a schematic sketch of a rectangular glades in the forest and a road which have no vegetation.

Figure 1b shows the FFM burning out and the formation of the fire temperature front. The temperature behind the back edge of the fire front gradually decreases. The fire front moves around the glades and spreads across the 20-meter-wide road (Fig 1c). Process duration is 35 min.

Figure 2 shows the results of numerical simulation of the process with the same initial situation, but in the absence of a wind. The fire front moves around the glades, but fails to cross the same 20-meter-wide road. Process duration is 1 h 55 min.

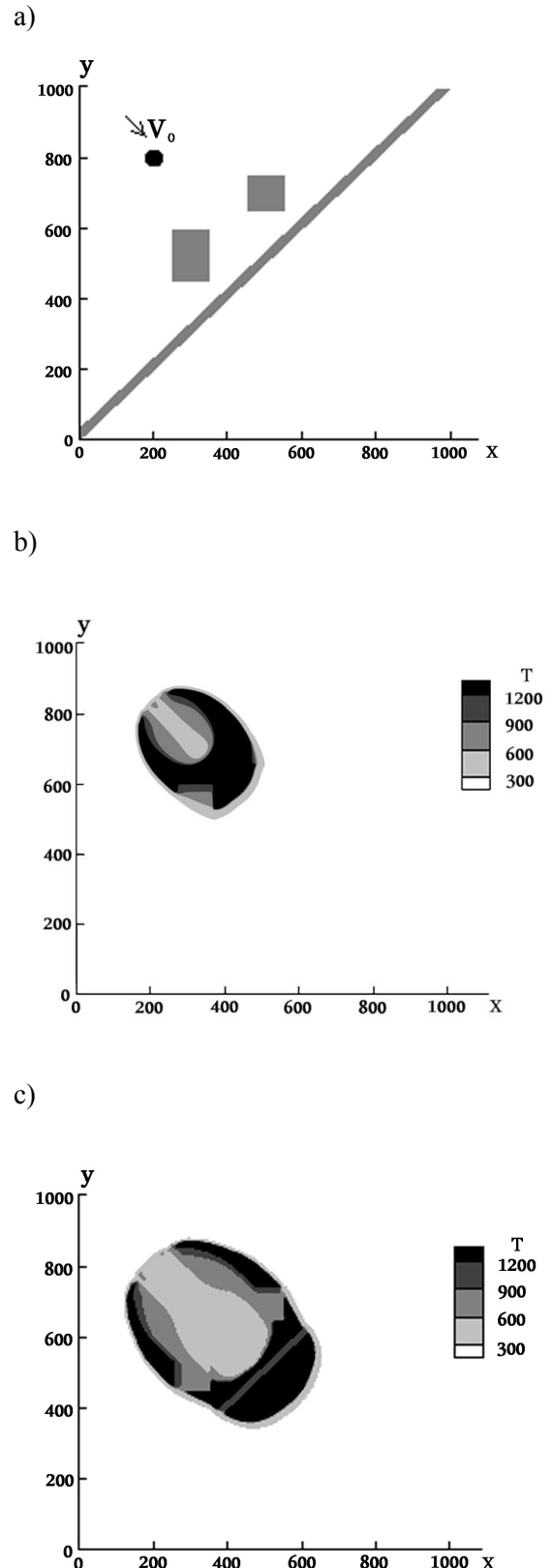
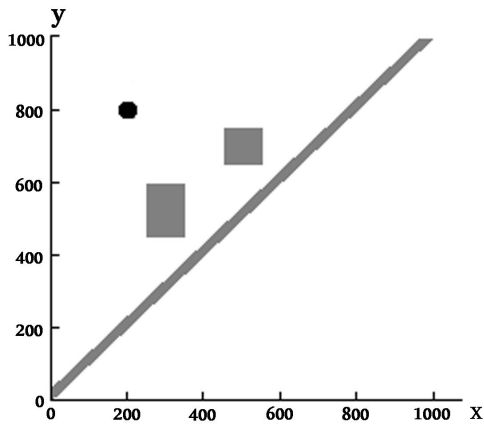
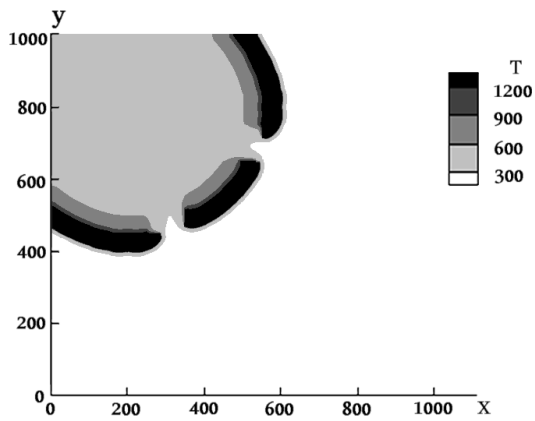


Fig. 1 The temperature front of the fire moves around the glades and across the 20-meter-wide road.

a)



b)



c)

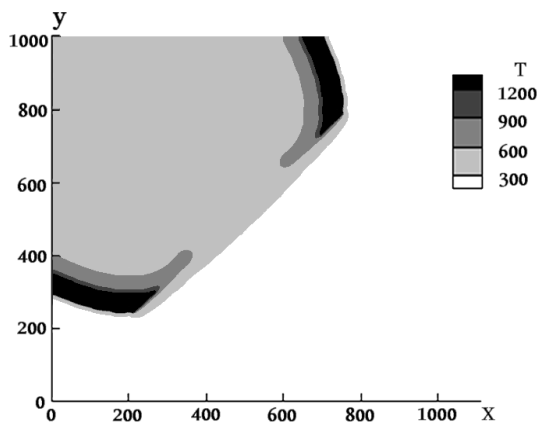
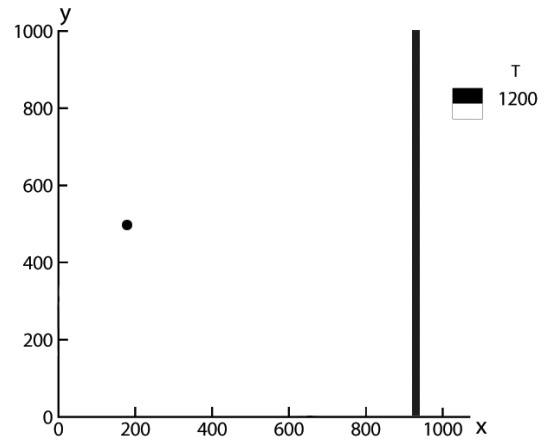


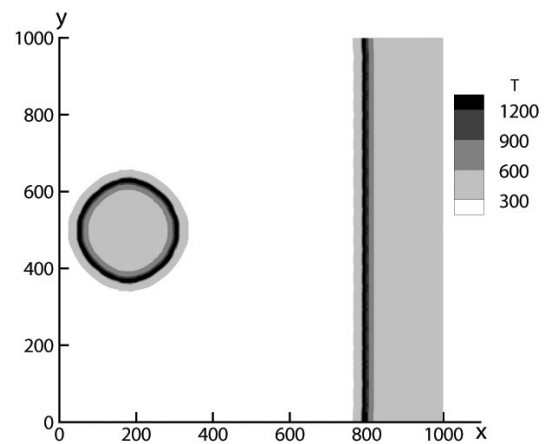
Fig. 2 The temperature front of the fire moves around the glades, but fails to cross the 20-meter-wide road.

On the Fig. 3 the results of computation of the back-fire are shown.

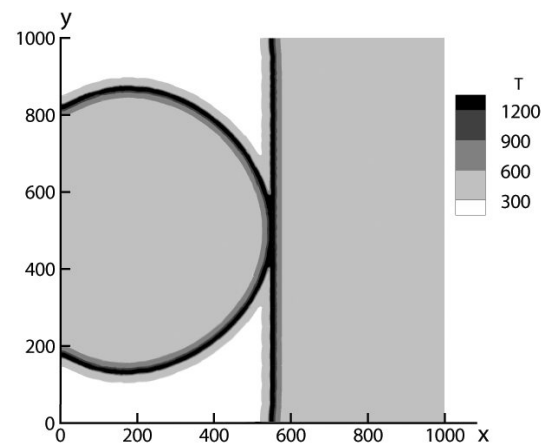
a)



b)



c)



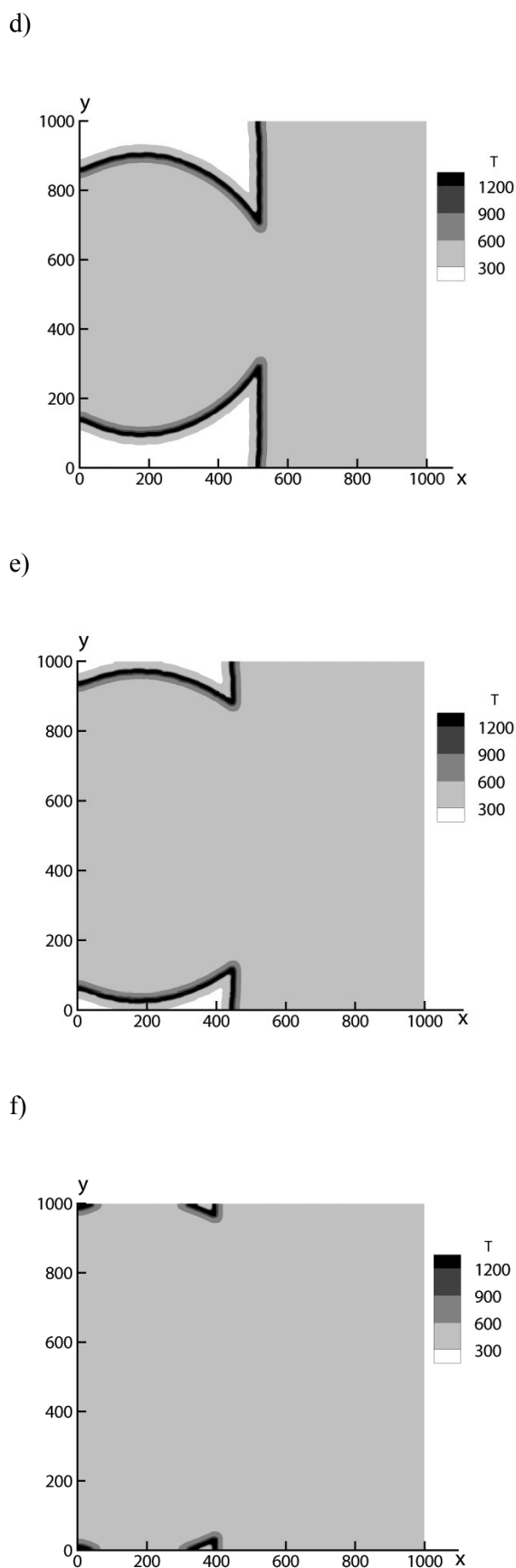


Fig. 3 The results of computation of the back-fire.

The fire fronts are moving from the opposite direction. As the result of the fire fronts interaction the fire dies out. Process duration is 1 h 41 min.

5 Conclusion

The results of numerical simulation are shown that the developed two-dimensional model correctly reflects the process of the fire front spreading for the case of non-homogeneous FFM distribution in the area, with such obstacles as roads, glades, water bodies etc., as well as in the presence of wind, i.e., for a particular set of conditions under which real forest fires occur.

References:

- [1] K. C. Clarke, J. A. Brass, P. J. Riggan, A cellular automaton model of wild firepropagation and extinction, *Photogramm. Eng Remote Sensing*, Vol. 60, 1994, pp. 1355–1367.
- [2] J. Quartieri, N. E. Mastorakis, G. Iannone, C. Guarnaccia, A Cellular Automata Model for Fire Spreading Prediction, *Latest Trends on Urban Planning and Transportation*, WSEAS Press, 2010, pp. 173-178.
- [3] A. M. Grishin, *Mathematical Modeling of Forest Fires and New Methods of Fighting Them*. Novosibirsk, Nauka Publishers, Siberian Division, 1992 (Russian).
- [4] B. Porterie, J. C. Loraud, D. Morvan, M. Larini, A numerical study of plumes in cross-flow conditions, *Int. J. Wildland Fire*, Vol.9, No.2, 1999, pp. 101-108.
- [5] R. Linn, J. Winterkamp, J. J. Colman, C. Edminster, J. D. Bailey, Modeling interactions between fire and atmosphere in discrete element fuel beds, *Int. J. Wildland Fire*, Vol.14, No.1, 2005, pp. 37-48.
- [6] P. Cunningham, S. L. Goodrick, M. Y. Hussaini, R. R. Linn, Coherent vertical structures in numerical simulations of buoyant plumes from wildland fires, *Int. J. Wildland Fire*, Vol.14, No.1, 2005, pp. 61–75.
- [7] T. L. Clark, M. A. Jenkins, J. L. Coen, D. R. Packham, A coupled atmosphere-fire model: role of the convective froude number and dynamic fingering at the fireline, *Int. J. Wildland Fire*, Vol.6, No.4, 1996, pp. 177-190.
- [8] T. L. Clark, J. L. Coen, D. Latham, Description of a coupled atmosphere-fire model, *Int. J. Wildland Fire*, Vol.13, No1, 2004, pp. 49–63.

- [9] J. L. Coen, Simulation of the Big Elk Fire using coupled atmosphere-fire modeling, *Int. J. Wildland Fire*, Vol.14, No.1, 2005, pp. 49-59.
- [10] A. A. Kuleshov, Mathematical forest fire models, *Mathematical modeling*, Vol.14, No.11, 2002, pp. 33–42 (Russian).
- [11] A. A. Kuleshov, E. E. Myshetskaya, Forest fire spread numerical simulation, *Proceeding of 5th WSEAS Int. Conference on Heat and Mass Transfer, Acapulco, Mexico, January 25-27, 2008*, WSEAS Press, 2008, pp. 151-155.
- [12] J. E. Penner, L. G. Haselman, L. L. Edwards, Buoyant plume calculations, 1985, Preprint AIAA, UCRL-90915.
- [13] B. N. Chetverushkin, *Mathematical Modeling of Radiant Gas Dynamics Problems*. Moscow, Nauka Publishers, 1985 (Russian).
- [14] Ya. B. Zeldovich, Yu. P. Raizer, *Physics of Shock Waves and High Temperature Hydrodynamic Phenomena*. Moscow, Fizmatgiz (Physics&Mathematics Publishers), 1963 (Russian).
- [15] M. E. Ladonkina, O. Yu. Milyukova, V. F. Tishkin, A Numerical Algorithm for Solving Diffusion-type Equations Based on the use of Multigrid Method, *Computational Mathematics and Mathematical Physics*, Vol.49, No.3, 2009, pp. 518-541.
- [16] M. E. Ladonkina, O. Yu. Milyukova, V. F. Tishkin, A Numerical Method for Solving Diffusion-type Equations Based on the use of Multigrid Method, *Computational Mathematics and Mathematical Physics*, Vol.50, No.8, 2010, pp. 1438-1461.